Agricultural and Forest Meteorology 343 (2023) 109782

Contents lists available at ScienceDirect

Agricultural and Forest Meteorology

journal homepage: www.elsevier.com/locate/agrformet

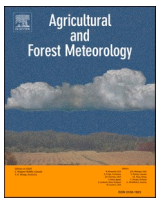

Non-stomatal processes are responsible for the decrease in gross primary production of a potato crop during edaphic drought

Quentin Beauclaire *, Bernard Heinesch, Bernard Longdoz

BIODYNE Biosystems Dynamics and Exchanges, TERRA Teaching and Research Center, Gembloux Agro-Bio Tech, University of Liège, Belgium

ARTICLE INFO

Keywords:
GPP
Eddy-covariance
Drought
Model
Potato
Stomatal conductance

ABSTRACT

Soil water stress is one of the main constraints on agrosystem functioning, causing a reduction in gross primary production (GPP). It is a key factor for the selection of drought-tolerant plant varieties and the adaptation of irrigation management strategies. Therefore, identifying the physiological factors limiting GPP is crucial. Land surface models commonly implement a beta (β) stress function to reproduce the effects of drought on GPP. It is still unclear whether GPP limitations originate from a direct stomatal response (SOL) or from other non-stomatal causes (NSOL). Moreover, the shape and thresholds of the β function are a major cause of uncertainty in LSMs. This study investigated the effects of edaphic drought on GPP limitations of a potato crop by using eddy covariance data from the Lonzée ICOS station (BE-Lon) in Belgium for four years (2006, 2010, 2014 and 2018) and by calibrating the β function on NSOL and SOL.

The decrease in the relative extractable water in the soil (REW) induced a decline in the apparent maximum carboxylation rate (NSOL) from similar REW thresholds for all growing seasons of potato crops. A sensitivity analysis showed that the non-inclusion of REW decrease on NSOL in the modeling of GPP led to important overestimations of carbon sequestration from a threshold corresponding to 46 % of the maximum available soil water. The stomatal sensitivity to photosynthesis (SOL) remained constant or even increased in 2010 and 2018. The carbon and water fluxes were decoupled when REW decreased, exhibiting a strict control of NSOL on hourly dynamics of GPP. This study provides REW thresholds to identify drought stress episodes and to help for designing irrigation management strategies. Our results advocate for a better representation of the influence of drought on photosynthesis processes of potato crops to improve the accuracy of model predictions during drought.

1. Introduction

Many regions across the world are facing more intense and frequent episodes of water stress due to climate change (Chiang et al., 2021). Edaphic drought has become a major limiting abiotic stress for agricultural production (Fahad et al., 2017). It is also known to cause restrictions in carbon assimilation, impacting the photosynthetic capacities of terrestrial ecosystems, especially those located in the mid-latitude region of the Northern Hemisphere (Yu et al., 2017). Consequently, severe water stress events reduce crop yield and sometimes offset carbon sinks or cause shifts from sink to source, inducing a positive feedback effect on global warming (Reichstein et al., 2013). Predicting and anticipating the impacts of drought on ecosystems' abilities to store carbon requires a detailed understanding of the physiological processes involving CO_2 uptake through photosynthesis and their interconnections.

Plants respond to low soil water content through a complex chain of mechanisms constituting their adaptation strategies (see Harper et al., 2021 for a review). For example, plants usually close their stomata when the atmospheric demand for water (represented by the vapor pressure deficit, VPD) overcomes the supply capacity from the soil, which prevents cavitation in the plants' hydraulic transfer system (Hetherington and Woodward, 2003). A consequence of stomatal closure is the reduction of CO_2 diffusion from the leaf-surrounding atmosphere to sub-stomatal cavities, which leads to a decrease in carbon assimilation (Flexas et al., 2004). Moreover, is it well known that stomatal conductance to CO_2 transfer (G_s) is highly correlated to gross primary production (GPP) under stable vapor pressure deficit and soil water status (Wong et al., 1979). These findings have been the basis of the empirical parametrization of G_s using carbon assimilation as a key element in

* Corresponding author.
E-mail address: q.beauclaire@uliege.be (Q. Beauclaire).

https://doi.org/10.1016/j.agrformet.2023.109782
Received 26 January 2023; Received in revised form 13 October 2023; Accepted 22 October 2023
Available online 31 October 2023

addition to environmental factors (see Damour et al., 2010 for a review). Within this framework, any decrease of G_s can be caused either by a modification of the environmental conditions or by an inhibition of photosynthetic capacities. The unified stomatal optimality (USO) model (Medlyn et al., 2011) reconciled this empirical approach with the optimality theory of Cowan and Farquhar (1977), which states that a plant should adjust its stomatal opening to maximize carbon assimilation while minimizing water losses over a constant time interval. In this USO framework, the G_1 parameter represents the slope of the linear relationship between G_s and carbon assimilation normalized by VPD and CO_2 concentration and is related to the marginal carbon gain per unit of water transpired (Medlyn et al., 2011). A reduction of carbon assimilation resulting from a decrease in G_1 corresponds to a direct stomatal control on CO_2 diffusion and will be referred in this paper to as a stomatal limitation of photosynthesis (SOL). Carbon assimilation can also be impacted in two possible ways: changes in mesophyll conductance restricting CO_2 diffusion from sub-stomatal cavities to the carboxylation sites in the chloroplast (Flexas et al., 2008), and inhibition of photosynthetic capacities. Both are generally implemented in photosynthesis modeling by a reduction of the apparent maximum carboxylation rate $V_{cmax,app}$ as in the Farquhar–von Caemmerer–Berry (FvCB) model (Farquhar et al., 1980; Flexas et al., 2004). This origin of CO_2 assimilation limitation is further associated in this paper to a non-stomatal limitation of photosynthesis (NSOL). It should be noted that NSOL also induces a diminution of G_s as carbon assimilation is recognized to be one of the variables influencing stomatal opening. The comparison between $V_{cmax,app}$ and G_1 dynamics during stressed periods gives insights on the importance of each cause of carbon photosynthesis perturbation (respectively NSOL and SOL). Using G_1 instead of G_s as an indicator of SOL allows to partition the coupling between G_s and GPP into changes in photosynthetic capacities and marginal water cost of carbon gain (Zhou et al., 2013, 2014).

Land surface models (LSMs) commonly implement a beta (β) stress function to account for soil water stress effects on carbon and water fluxes. This function uses the soil water content (SWC) normalized by the difference between the field capacity and the wilting point in the root layer (Egea et al., 2011) to characterize the amount of water available for plant uptake. When SWC is below the field capacity, the β factor directly downregulates $V_{cmax,app}$ and/or G_1 (Egea et al., 2011; Verhoef and Egea, 2014) to reproduce drought effects on carbon and water fluxes originating from respectively NSOL and SOL. However, Granier et al. (1999) and Gourlez de la Motte et al. (2020) showed that ecosystems can maintain a high level of carbon and water flux even when SWC is below the field capacity, leading to potential underestimations in flux estimates from LSMs. Vidale et al. (2021) and Trugman et al. (2018) underlined this aspect by identifying that this stress function was one of the key uncertainties in photosynthesis and transpiration predictions in LSMs. Moreover, there is no consensus in the scientific community on whether soil water stress should impact stomatal functioning, photosynthetic capacities, or both, to accurately predict carbon and water fluxes during drought (Zhou et al., 2013; Peters et al., 2018). Therefore, the determination of the β stress factor (corresponding to a REW function) representing NSOL and SOL for different plant functional types (PFT) is a key factor for improving model predictions (Rodgers et al., 2017; Li et al., 2022).

Potato (*Solanum tuberosum*) is the third most important crop in the world in terms of food production, with more than 370 million metric tons produced in 2019 (FAOSTAT, 2021). In Europe, most potato crops are cultivated on loam soils with a predominance of clay, which allows the soil to hold an important amount of water for plant uptake. Potatoes cultivated on these soils represent more than 400 000 hectares of arable lands in Europe (Goffart et al., 2022). Known to be a drought sensitive crop because of its shallow root system, potato yield and the quality of the tuber can be dramatically impacted by water stress (Obidiegwu, 2015). Therefore, any limitation on its production threatens food supply, impacting more than one billion people around the world (Lutaladio and Castaidi, 2009).

Up to now, no studies have investigated which processes are at the origin of the effects of drought on potato photosynthesis limitations estimated from eddy covariance data (EC). In this paper, we aimed at investigating the effects of drought on potato carbon assimilation by analyzing the data collected by the Lonzée flux tower and meteorological station (BE-Lon) located in central Belgium, which is part of the Integrated Carbon Observation System (ICOS – Franz et al., 2018). More specifically, this paper aims at: (i) partitioning the impacts of REW on GPP between SOL (G_1) and NSOL ($V_{cmax,app}$) and (ii) defining a REW threshold below which these two limitations occurred.

2. Materials and methods

2.1. Site description

The Lonzée ICOS flux tower (Level 2 ICOS station) is installed in the middle of a cropland located in Lonzée, about 50 km SE of Brussels in Belgium (50°33′5.71″N, 4°44′46.07″E, 167 m asl). It has been equipped with an eddy covariance (EC) system and a meteorological station since 2004 and is integrated into the CarboEurope-IP and FLUXNET networks. The cropland plot has an area of 12 hectares. The EC system has a fetch of 240 m and 200 m in the directions of the prevailing winds which are SW and NE (Buysse et al., 2017). For any atmospheric conditions, the cropland area contribution to the EC footprint fluxes was large (91.1 % in 2006, 90.5 % in 2010, 90.7 % in 2014, 93.3 % in 2018 – data not shown). The climate is temperate oceanic, with mean annual temperature and precipitation of respectively 10.2 °C and 743 mm. The soil is a Luvisol (FAO classification) divided into two horizons (one plow layer from 0 to 35 cm and one layer enriched in clay particles from 35 to 100 cm – Table 1).

2.2. Crop management

The Lonzée station has been cultivated for more than 80 years, with cropping management based on a 4-year rotation. For at least the past 20 years (Aubinet et al., 2009), the rotation has been: winter wheat (*Triticum aestivum*) / sugar beet (*Beta vulgaris*) / winter wheat (*Triticum aestivum*) / seed potato (*Solanum tuberosum*). Potatoes were cultivated in 2006, 2010, 2014 and 2018. The farming operations during the four growing seasons are described in Table S1. The tubers were planted in ridges with a space of 60 to 70 cm between the ridges and of 30 to 40 cm between the tubers.

2.3. Meteorological and fluxes measurements

Micrometeorological measurements were collected at the half-hourly timescale, including air humidity and air temperature (RHT2, Delta-T Devices Ltd., Cambridge, UK) at 1.3 m height (and 2.8 m height in 2018), incident photosynthetic photon flux density (PAR Quantum sensor SKP 215, Skye Instruments Limited, Llandrindod Wells, UK) and SWC (EnviroSCAN Probe, Sentek Sensor Technologies, Stepney, SA, AU) at five different depths in 2018 (5, 15, 25, 55 and 85 cm). In 2006, 2010

Table 1
Soil physical proprieties of the BE-Lon EC site: field capacity (θ_{fc}), wilting point (θ_{wp}), sand, silt, clay content and bulk density for the two soil horizons (0–35 cm and 35–100 cm). Field capacities and wilting points were measured by the WPC4 and HYPROP2 sensors (Meter environment., Hopkins Ct, NE, US) on soil samples collected in 2019.

Depth (cm)	θ_{fc} (cm^{-3} cm^{-3})	θ_{wp} (cm^{-3} cm^{-3})	Sand (%)	Silt (%)	Clay (%)	Bulk density (g cm^{-3})
0–35	45.3	11.7	8.4	80.5	11.2	1.3
35–85	40.4	13.0	6.1	75.7	18.2	1.5

and 2014, SWC was measured using time domain reflectometers (ML2 ThetaProbe, Delta-T Devices Ltd, Cambridge, UK) at three different depths (5, 20 and 40 cm). For all years, the soil water sensors were located at the middle of the plot near the EC station.

The net CO_2 (F_c) and water vapor (*LE*) fluxes between the ecosystem and the atmosphere were determined on a half-hourly basis by the EC technique (Aubinet et al., 2012) using high frequency data of vertical wind speed, CO_2 and water vapor concentrations at the ecosystem-atmosphere interface. These variables were measured at 20 Hz by respectively a sonic anemometer (Solent Research R3, Gill Instruments Lymington, UK) placed at a height of 2.93 m on a mast located at the center of the field, and an infrared gas analyzer (LI-7000 before 2014 and LI-7200 after, LI-COR, Lincoln, NE, US) placed close to the anemometer. Half-hourly fluxes of F_c and LE were determined by post-processing raw 20 Hz data by the ICOS Ecosystem Thematic Center using the ONEFlux pipeline (Pastorello et al., 2020) and are available in the ICOS Carbon Portal (Heinesch et al., 2022). More precisely, the storage flux was neglected (i.e., F_c corresponds to the net ecosystem exchange *NEE*) and GPP was obtained from the partitioning of *NEE* using the nighttime method (NT, Reichstein et al., 2005). Moreover, data characterized by weak atmosphere turbulence level (low friction velocity u^*) using the variable u^* threshold method (VUT) were discarded. The variables GPP_NT_VUT_REF and LE_F_MDS with quality flags of 0 were selected from the dataset. Data was not gapfilled because only measurements can be used to study ecosystem functioning and no flux value cumulated over time were necessary.

2.4. Measurements of vegetation growth

Vegetation growth is commonly measured by the leaf area index (LAI) which corresponds to the ratio of leaf area to unit ground surface area (Breda et al., 2003). However, the LAI does not allow to separate the green photosynthetic components (including chlorophyll cells) from the rest of the canopy structure. The green area index (GAI), which corresponds to the green surface area of the vegetation, is a better proxy to assess the photosynthetically active component of the ecosystem. In this study, the GAI of the potato crop was measured six times during each growing season by a destructive sampling method. These measurements have been linked to the growing degree-days which is a main climatic driver of crop development (Mcmaster, 1997). The base temperature (temperature required for crop growth) was set to 7 °C (Sands et al., 1979). A third-order polynomial function was fitted to GAI and growing-degree-days to model GAI dynamics and get a continuous function for each growing seasons.

In the results section, the timescale will be further expressed as "day after emergence" (DAE), which counts the number of days after the emergence of the first leaves of the crop, this latter corresponding to the date when GAI changed from a null to a positive value. The growing seasons were divided into two stages: the vegetative stage when GAI increased (leaf development and period before tuber development, roughly between DAE 0 and 40), and the reproductive stage when GAI decreased (tuber multiplication and elongation, roughly after DAE 40). This definition slightly differs from the reality since tuber growth initiation is expected to start before GAI reaches its maximum value (Obidiegwu, 2015). However, this assumption will not affect the results of this study since this denomination was only used for a descriptive purpose.

2.5. Quantification of soil water availability

The relative extractable water (*REW*) for plant uptake is a drought index which corresponds to the fraction of available water for plant uptake from the soil surface up to the maximum rooting depth. *REW* is expressed as a fraction of the maximum available water calculated by the difference between field capacity and wilting point (Granier et al., 1999). The maximum rooting depth was estimated by analyzing the dynamics of SWC within each soil horizon during periods of potato crop development without precipitation. The decrease in SWC was observed only within the first soil horizon (0–35 cm, Table 1), suggesting that root water uptake only occurred in surface soil layers. Therefore, we assumed that the roots can uptake soil water only up to 35 cm depth (Table 1). This assumption could lead to *REW* overestimation at the beginning of the growing season as most roots are located within shallow soil layers. However, SWC data showed a rapid extension of the water uptake into deeper soil layers and the beginning of the growing season is not a drought-prone period. *REW* was calculated as follows (Granier et al., 1999):

$$REW = \left\{ \frac{\overline{\theta} - \theta_{wp}}{\theta_{fc} - \theta_{wp}} \right. \quad (1)$$

where θ_{wp}, θ_{fc} and $\overline{\theta}$ are respectively the wilting point, the field capacity and the average of SWC measurements in the first soil horizon (Table 1). The units and a description of the variables used in this study can be found in Table S2. *REW* ranges from 1 ($\overline{\theta} = \theta_{fc}$) to 0 ($\overline{\theta} = \theta_{wp}$), even if values higher than 1 can be observed just after a rainfall event, when soil water content is above field capacity. *REW* is directly related to the water stress β factor used in many LSMs (Verhoef and Egea, 2014):

$$\beta = \begin{cases} 1, & \overline{\theta} > \theta_{fc} \\ REW^p, & \theta_{wp} < \overline{\theta} < \theta_{fc} \\ 0, & \overline{\theta} < \theta_{wp} \end{cases} \quad (2)$$

with p the exponent allowing to implement a non-linear dependence of model parameters on *REW*. However, many species can maintain constant photosynthetic parameters even when $\overline{\theta} < \theta_{fc}$ (Granier et al., 1999; Gourlez de la Motte et al., 2020). Investigating the effects of drought on SOL and NSOL to determine specific *REW* thresholds from which model parameters linked to stomatal opening and apparent carboxylation rate are impacted by water stress is pivotal to avoid the propagation of uncertainties in models. This study focused on the characterization of these threshold by assuming that $p = 1$, as implemented in many LSMs (Vidale et al., 2021; Oliver et al., 2022).

2.6. "Big-leaf" approach

The "big-leaf" is a concept where the canopy is simplified as a single leaf at the interface with the surrounding atmosphere. It is used to infer ecosystem physiological proprieties from flux tower measurements (Knauer et al., 2018a). The air characteristics over the "big-leaf" surface and the conductance related to the transfer of water vapor through respectively the stomata of the "big-leaf" (named canopy conductance to water vapor G_{sw}) and the boundary layer (named aerodynamic conductance to water vapor G_{aw}) can be inferred from the micro-meteorological measurements performed above the canopy.

2.6.1. Determination of the "big-leaf" surface conditions and aerodynamic conductance

Following the Thom model (Thom, 1972), G_{aw} is equivalent to the aerodynamic conductance for sensible heat (G_{ah}) and can be determined by:

$$G_{aw} = G_{ah} = \left(\frac{u}{u_*^2} + 6u_*^{-0.667} \right)^{-1} \quad (3)$$

where u_* is the friction velocity and u the wind speed above the canopy. G_{ah} was used to calculate the H_2O concentration (e_s) and the CO_2 concentration (C_s) at the "big-leaf" surface as follows (Knauer et al., 2018a):

$$e_s = e_a + \frac{LE\ \gamma}{\rho_a\ G_{aw}\ c_p} \quad (4)$$

$$C_s = C_a + \frac{NEE}{G_{aw}} \frac{R\,T_a}{p} \quad (5)$$

with LE the latent heat flux (measured by the EC system), ρ_a the air density, c_p the heat capacity of dry air, γ the psychrometric constant and R is the perfect gas constant. e_a, C_a, T_a and p correspond respectively to the air vapor pressure, the CO_2 concentration, the air temperature and the air pressure measured above the canopy. $\frac{R\,T_a}{p}$ in Eq. (5) converts G_{aw} from m s^{-1} to mol m^{-2} s^{-1}.

The canopy temperature was determined from the longwave fluxes at the canopy surface (Knauer et al., 2018a):

$$T_s = \sqrt[4]{\frac{LW_{out} - (1-\varepsilon)LW_{in}}{\varepsilon\,\sigma}} \quad (6)$$

with LW_{in} and LW_{out} the longwave downward and outgoing fluxes measured by the meteorological station, ε the emissivity of the canopy and σ the Stefan-Boltzmann constant. Missing T_s values due to lack of longwave fluxes measurements were gap filled with T_a. The vapor pressure deficit at the "big-leaf" surface (VPD_s) was calculated as the difference between the saturated vapor pressure and the air vapor pressure at the canopy surface (e_s).

2.6.2. Canopy conductance

G_{sw} was computed by inverting the Penman-Monteith equation (Monteith, 1965):

$$G_{sw} = \frac{G_{ah}\,\gamma\,LE}{\Delta\,(R_n - G - S) + \rho_a\,c_p\,G_{ah}\,VPD_s - (\Delta+\gamma)\,LE} \quad (7)$$

where Δ is the slope of the saturated vapor pressure curve at T_a calculated from Allen et al. (1998), R_n is the net radiative flux and G the ground heat flux (both measured). The flux corresponding to the energy stored in the canopy (S) was neglected. Inferring G_{sw} from Eq. (7) is only possible when LE corresponds to the transpiration flux of the ecosystem (i.e., when soil and canopy evaporation are negligible comparing to transpiration). Therefore, the analysis focused only on the growing season and data during precipitation events and the subsequent 48 h (when evaporation is significant) were discarded. To ensure the selection of data with meaningful LE values, periods with low photosynthetic photon flux density (PPFD< 200 μmol m^{-2} s^{-1}), low surface temperature (<5 °C), high relative humidity (RH>95 %), $LE < 0$ and $R_n - G < 0$ were also discarded (Knauer et al., 2018b). Moreover, the violation of the energy balance closure assumption in Eq. (7) may affect the interpretability of G_{sw} (Knauer et al., 2018b). This issue was addressed by computing the slope of the regression between the sum of the turbulent fluxes ($LE + H$) and available energy ($R_n - G$) and by discarding half hourly data when the standardized residuals from the linear regression between $LE + H$ and $R_n - G$ were superior to 3.

2.6.3. Maximum apparent carboxylation rate

Under high irradiance, photosynthesis is limited by the activity of the RuBisCO enzyme (Farquhar et al., 1980). In this case, the FvCB model applied at the "big leaf" surface estimates GPP under high irradiance (GPP_{sat}) from the apparent maximum carboxylation rate ($V_{cmax,app}$), the intracellular CO_2 concentration (C_i,), the CO_2 compensation (Γ^*) point and the effective Michaelis-Menten coefficient for RuBisCO kinetics (K_m):

$$GPP_{sat} = \frac{V_{cmax,app}(C_i - \Gamma^*)}{C_i + K_m} \quad (8)$$

Both K_m and Γ^* were determined following an air temperature-based dependence (Bernacchi et al., 2001). Eq. (8) assumes that leaf photorespiration is negligible under high irradiance. $V_{cmax,app}$ was calculated by inverting Eq. (8):

$$V_{cmax,app} = GPP_{sat}\frac{C_i + K_m}{C_i - \Gamma^*} \quad (9)$$

where GPP_{sat} is the GPP when PPFD is higher that a threshold ($PPFD_{sat}$) from which GPP saturated. This threshold was calculated from the light response curves of GPP for each growing season. The Mitscherlich model was used to mathematically describe the relationship between GPP and PPFD. Data was averaged within classes with a constant width of 200 μmol$m^{-2}s^{-1}$ (respectively $\overline{GPP}$ and $\overline{PPFD}$):

$$\overline{GPP} = a\left(1 - e^{-b(\overline{PPFD}-c)}\right) \quad (10)$$

with a, b and c three parameters to adjust. The PPFD threshold was defined as the PPFD value when GPP deviated from the asymptote of the model (a) as follows:

$$PPFD_{sat} = c - \frac{ln\left(\frac{SE_a}{a}\right)}{b} \quad (11)$$

with SE_a the standard deviation around a. In Eq. (9), C_i was determined following a Fick diffusive law (Farquhar and Sharkey, 1982), representing the CO_2 diffusion through stomata:

$$C_i = C_s - \frac{1.6\,GPP_{sat}}{G_{sw}} \quad (12)$$

where G_{sw} is determined by Eq. (7), 1.6 is the ratio between H_2O and CO_2 conductances and C_s is the CO_2 concentration at the leaf surface, determined based on Eq. (5). $V_{cmax,app}$ values were further normalized at 25 °C ($V_{cmax,app,25}$) by adjusting the Arrhenius model on $V_{cmax,app}$ and T_s data averaged within T_s classes with a width of 2 °C (Medlyn et al., 2002).

2.7. NSOL during drought

The effects of drought on NSOL can be characterized only if the influence of other factors on the dynamics of $V_{cmax,app}$ is discarded from the analysis. The impact of u_* is limited by selecting fluxes during low turbulence periods, while $V_{cmax,app}$ was normalized at 25 °C to account for temperature effects on NSOL. Moreover, only half-hourly data at high irradiance (PPFD higher than $PPFD_{sat}$) were selected. The only remaining potential influence (besides REW) comes from the GAI variability which can be observed only for a study of the seasonal dynamics of GPP_{sat}. Therefore, the analysis should be focused on periods with relatively low variations of the phenological development of the crop. To overcome this potential influence, data with GAI above a threshold (GAI_{sat}) were selected to ensure that the amount of green area is high enough so that any increase in the green canopy cover had a negligible effect on GPP_{sat} dynamics. GAI_{sat} was determined by the same method as $PPFD_{sat}$ using Eqs. (10) and (11) by replacing PPFD by GAI. Days when GAI<GAI_{sat} were discarded since it may induce a bias in the analysis of the influence of REW on SOL and NSOL. The impact of edaphic drought on GPP originating from NSOL was assessed by studying the influence of REW on $V_{cmax,app,25}$ using the data selected.

2.8. SOL during drought

SOL was defined in this paper as a decrease in G_1, the slope parameter of the USO model which was adapted from the leaf to the canopy level by using the "big-leaf" framework (Medlyn et al., 2017; Knauer et al., 2018a):

$$G_{sw} = G_0 + 1.6\left(1 + \frac{G_1}{\sqrt{VPD_s}}\right)\frac{GPP_{sat}}{C_s} \quad (13)$$

where G_0 is the minimum stomatal conductance which was set to

0 (Medlyn et al., 2017) and G_1 represents the ecosystem stomatal sensitivity to GPP at high irradiance normalized by VPD_s and C_s. G_1 was calculated by combining Eqs. (12) and (13):

$$G_1 = \frac{\frac{C_i}{C_s}\sqrt{VPD_s}}{1-\frac{C_i}{C_s}} \quad (14)$$

The impact of edaphic drought on GPP_{sat} originating from SOL was assessed by studying the influence of *REW* on G_1.

2.9. Detection of REW thresholds

A linear segmented model including one breakpoint and one segment at a constant value for high *REW* (asymptote) was adjusted between half-hourly $V_{cmax,app,25}$ or G_1 and *REW*. The asymptote of the model characterizes the unstressed $V_{cmax,app,25}$ and G_1 values, respectively named $V_{cmax,app,25}{}^*$ and $G_1{}^*$.This procedure allows the detection of a breakpoint, below which SOL and NSOL increase or decrease linearly with *REW*. A Fisher F-test was conducted to verify if this segmented model was significantly different from a linear regression with no breakpoint. The quality of the segmented regressions was also assessed by the p-values of the adjusted coefficients and the R^2 of the model.

2.10. Sensitivity analysis

A sensitivity analysis was performed by calculating the ratio between theoretical GPP_{sat} values that would be modeled without accounting for water stress effect on $V_{cmax,app,25}$ and G_1 ($GPP_{Vcmax,app,25}{}^*$ and $GPP_{G1}{}^*$), with observed GPP_{sat} values. $GPP_{Vcmax,app,25}{}^*$ was determined by using Eq. (8) where $V_{cmax,app,25}$ was replaced by $V_{cmax,app,25}{}^*$ and by assuming that G_0 and ecosystem respiration are negligible. C_i in Eq. (8) was deduced from $GPP_{Vcmax,app,25}{}^*$, C_a, G_{aw}, G_1 and VPD_s by combining Eqs. (12), (5) and (13):

$$C_i = \left(C_a - \frac{GPP_{Vcmax,app,25}{}^*}{G_{aw}}\right)\left(1 - \frac{1}{\left(1+\frac{G_1}{\sqrt{VPD_s}}\right)}\right) \quad (15)$$

Inserting Eq. (15) in Eq. (8) gives the following equation:

$$GPP_{Vcmax,app,25}{}^* = V_{cmax,app,25}{}^* \frac{\left(C_a - \frac{GPP_{Vcmax,app,25}{}^*}{G_{aw}}\right)\left(1 - \frac{1}{\left(1+\frac{G_1}{\sqrt{VPD}}\right)}\right) - \Gamma^*}{\left(C_a - \frac{GPP_{Vcmax,app,25}{}^*}{G_{aw}}\right)\left(1 - \frac{1}{\left(1+\frac{G_1}{\sqrt{VPD}}\right)}\right) + K_m} \quad (16)$$

which was solved for $GPP_{Vcmax,app,25}{}^*$. In a similar way, $GPP_{G1}{}^*$ was determined by solving Eq. (16) where $V_{cmax,app,25}{}^*$ was replaced by observed $V_{cmax,app,25}$ and G_1 by $G_1{}^*$. The comparison between $GPP_{Vcmax,app,25}{}^*$ (or $GPP_{G1}{}^*$) and the measured GPP_{sat} estimates the bias induced by the non-inclusion of NSOL (or SOL) in the modeling of GPP_{sat} . More precisely, a ratio $GPP_{G1}{}^*/GPP_{sat}$ or $GPP_{Vcmax,app,25}{}^*/GPP_{sat}$ higher than 1 indicates an overestimation of GPP_{sat} when *REW* effects on G_1 or $V_{cmax,app,25}$ are not considered.

2.11. Coupling between transpiration and photosynthesis

Stomata opening regulates both CO_2 and water vapor fluxes and is affected by the evaporative demand of the atmosphere. This leads to a high degree of coupling at the hourly timescale between $GPP\sqrt{VPD_s}$ and *LE* (Nelson et al., 2018). Changes in environmental conditions may affect this level of coupling. Temperature variations, or appearance of cloud cover (decrease of PPFD) may induce a decoupling between $GPP\sqrt{VPD_s}$ and *LE* (Reinhardt and Smith, 2008; Urban et al., 2017; Kirch et al., 2022; Marchin et al., 2022). Moreover, as drought intensifies and affects biochemical factors, carbon fixation may inhibited independently from transpiration, resulting in a decrease in $GPP\sqrt{VPD_s}$ independently of *LE*. Therefore, avoiding the potential effects of PPFD and T_s is required to investigate the effects of drought on the coupling between $GPP\sqrt{VPD_s}$ and *LE*. This has been realized by regrouping many days with large ranges of T_s and PPFD daily variations.

The level of coupling was quantified by the Spearman's rank correlation coefficient (Spearman, 1904) between *LE* and normalized carbon assimilation ($GPP\sqrt{VPD_s}$) (Nelson et al., 2018):

$$DWCI = \rho\left(LE, GPP\sqrt{VPD_s}\right) \quad (17)$$

with *DWCI* the Diurnal Water-Carbon Index (Nelson et al., 2018). The fluxes were normalized by their maximum value for each day before using Eq. (17), which allowed for using fluxes measurements across growing seasons. The data already discarded for the G_{sw} calculation process was removed, and the period of analysis was restricted to the growing seasons. A linear segmented regression was adjusted on the *DWCI* dependence on *REW* (all years regrouped) following the method presented in 2.9 to detect if the decrease in *REW* impacted the degree of coupling between carbon and water fluxes.

3. Results

3.1. Ancillary data and photosynthesis dynamics

3.1.1. Crop characteristics and pedo-climatic conditions

The maximum GAI value was measured in 2010 (5.02) while other years showed relatively similar maximum values between 3 and 4 (Fig. 1, Table 2). The year 2006 had the longest growing season with 74 days, compared to the three other years, which had a growing season of 71 days in 2010, 64 days in 2014 and 66 days in 2018 (Table 2). These differences are explained by farming activities and haulm killing dates that change throughout the years.

The 2018 growing season had the lowest rainfall, with cumulative precipitation of 68.4 mm, slightly lower than 2010 (76.6 mm), and considerably below 2006 (186.2 mm) and 2014 (222.4 mm) (Table 2). In 2018, the site was irrigated two times (24.5 mm) by the aspersion technique (Fig. 1), for a total amount of water received by the crop of about 92.9 mm (precipitation and irrigation). SWC at 5 cm depth decreased with the lack of precipitation and reached approximately 16 % in 2018 and 2010 (Fig. 1), which was slightly higher than the wilting point (θ_{wp} =11.7 between 0 and 35 cm depth– Table 1). The minimum SWC values at deeper depths remained close to 25 %, suggesting that deeper soil layers in the first horizon were able to hold water above the wilting point during the growing seasons. The periods of lack of precipitation were associated to an increase in VPD_s and T_s (regularly in 2010, in late 2006 and 2018) when their daily averaged values both reached respectively about 1.5 kPa and 25 °C (Fig. 1). The trends in VPD_s, T_s and SWC illustrated that climate conditions generated periods with potential conditions for both atmospheric and edaphic droughts during the vegetative stage in 2010 and during the reproductive stage in 2006 and 2018. The lowest REW values were quite similar in 2006, 2010 and 2018 growing seasons at respectively 0.40, 0.31 and 0.30 (Fig. 2). In 2014, *REW* was always higher than 0.60 due to favorable weather conditions.

3.1.2. Photosynthesis and canopy conductance dynamics

A deviation from the expected bell-shape GPP_{sat} curve following GAI dynamics can be observed in 2018 and 2006 (during the reproductive stage) and in 2010 (during the vegetative stage) where GPP_{sat} dropped from 25 to 35 μmol m^{-2} s^{-1} to 5–15 μmol m^{-2} s^{-1} (Fig. 2). These sharp

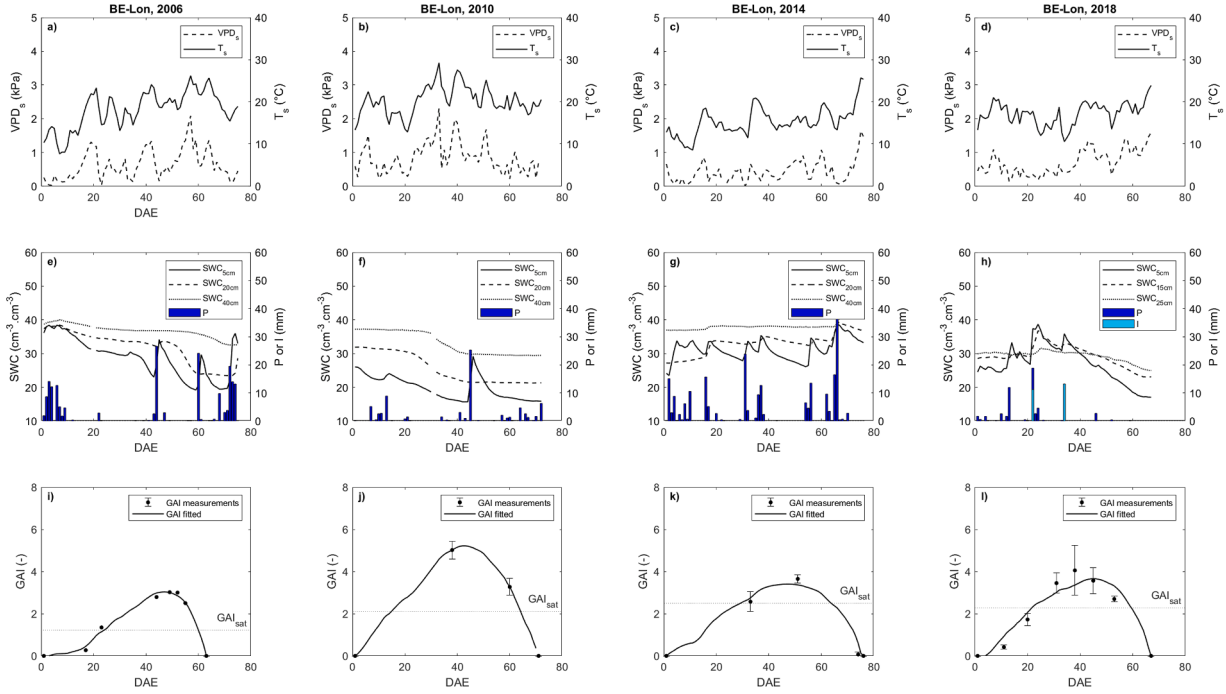

Fig. 1. Vapor pressure deficit at the canopy surface (VPD_s), canopy temperature (T_s) (subplots a to d) and soil water content (SWC) (subplots e to h) daily means. Daily sums of precipitation (P) and irrigation (I) are displayed on the second line (subplots e to h). Interpolated green area index GAI (GAI fitted) and measurements (GAI measurements) with their standard deviation are shown on the third line (subplots i to l). DAE corresponds to days after emergence.

Table 2
Crop characteristics: growing season (from emergence to haulm killing), cumulative precipitation (P_{cum}), irrigation (I), maximum green area index (GAI_{max}) and variety.

	Growing season (days)	P_{cum} (mm)	I (mm)	GAI_{max} (-)	Variety (% of total area)
2006	74	186.2	–	3.02	Spunta (62.8%) / Primura (11.6%) / Kondor (11.6%) / Draga (14%)
2010	71	76.6	–	5.02 ± 0.42	Draga (100%)
2014	64	222.4	–	3.55 ± 0.19	Draga (72.8%) / Bianchidea (20%) / Kennebec (7.2%)
2018	66	68.4	24.5	4.05 ± 1.18	Agria (53.9%) / Unidea (26.4%) / Draga (19.7%)

declines coincided with the decrease in *REW* (roughly from 0.65 to 0.45 in 2006, and from 0.60 to 0.30 in 2010 and 2018) and G_{sw} (roughly from 0.60 to 0.25 mol m^{-2} s^{-1} in 2006 and from 0.25 to 0.10 mol m^{-2} s^{-1} in 2010 and 2018, Fig. 2), which corresponded to the closure of the stomata when *REW* values were low. The relatively small amount of data recorded in 2014 (due to numerous precipitation events, and important gaps in the shortwave and longwave flux measurements) and 2006 (due to numerous days when cumulative precipitation was very low; e.g., <0.3 mm day^{-1} on DAE 39, 41, 56 or 64) explain that very few G_{sw} data points were available for the analysis. These observations highlighted two different timings in drought appearance with varying amplitude and intensity, characterized by a decrease in GPP_{sat} and G_{sw}.

3.2. Drought impact on SOL and NSOL at the seasonal scale

3.2.1. Impact of drought on $V_{cmax,app,25}$

$V_{cmax,app,25}$ decreased with the decline in *REW*. The linear segmented model significantly described the dependence between $V_{cmax,app,25}$ and *REW* in 2018, 2010 and 2006 (Table 3 – Fig. 3). *REW* breakpoints ranging between 0.58 ± 0.01 and 0.45 ± 0.02 were found whatever the development stages of the crop when drought occurred, indicating a relatively uniform tipping point below which the photosynthetic capacities of the canopy decrease due to edaphic drought (Table 3). The asymptote of the model ($V_{cmax,app,25}$*) or averaged value was in a narrow range (from 98.7 ± 1.69 µmol m^{-2} s^{-1} in 2018 to 128 ± 6.11 µmol m^{-2} s^{-1} in 2010 – Table 3). In 2014, no effect of *REW* on $V_{cmax,app,25}$ was observed due to recurrent precipitation events and reduced amount of data (see explanation above). The slopes of the linear segmented model ranged from 324 ± 36.2 µmol m^{-2} s^{-1} in 2018 to 821 ± 137 µmol m^{-2} s^{-1} in 2010). The systematic pattern of decreasing $V_{cmax,app,25}$ with *REW* with quite similar unstressed values and breakpoints whatever the years demonstrated the existence of a clear uniform dependence of photosynthetic capacities on soil water availability either during the vegetative (2010) or reproductive stage (2006 and 2018).

3.2.2. Impact of drought on G_1

G_1 was significantly impacted by *REW* in 2010 and 2018. More precisely, G_1 increased during respectively the vegetative and reproductive stages (Fig. 3). The *REW* breakpoints were very similar for these two years (0.44 ± 0.05 in 2010 and 0.45 ± 0.03 in 2018, Table 3, Fig. 3). The asymptote value was slightly higher in 2010 (1.69 ± 0.24 $kPa^{0.5}$) compared to 2018 (2.37 ± 0.05 $kPa^{0.5}$). No significant effect of *REW* on G_1 was observed in 2006 and 2014. The averaged G_1 values in 2006 and 2014 (4.35 ± 0.80 $kPa^{0.5}$ and 4.44 ± 1.45 $kPa^{0.5}$ respectively, Table 3) were clearly higher than the asymptote of the segmented model in 2010 and 2018.

3.2.3. Impact of drought on GPP modeling

$GPP_{Vcmax,app,25}$*/GPP_{sat} increased when *REW* passed below a *REW* breakpoint of 0.46 ± 0.01 for all years when edaphic drought induced NSOL, which is logically a similar breakpoint compared to those for $V_{cmax,app,25}$ (Fig. 4- Table 3). This ratio even exceeded 2 in 2010 and 2018 when the *REW* reached its minimum values during water stress events (Fig. 4). In opposition, the ratio GPP_{G1}*/GPP_{sat} remained relatively constant for all the years and whatever the soil water availability

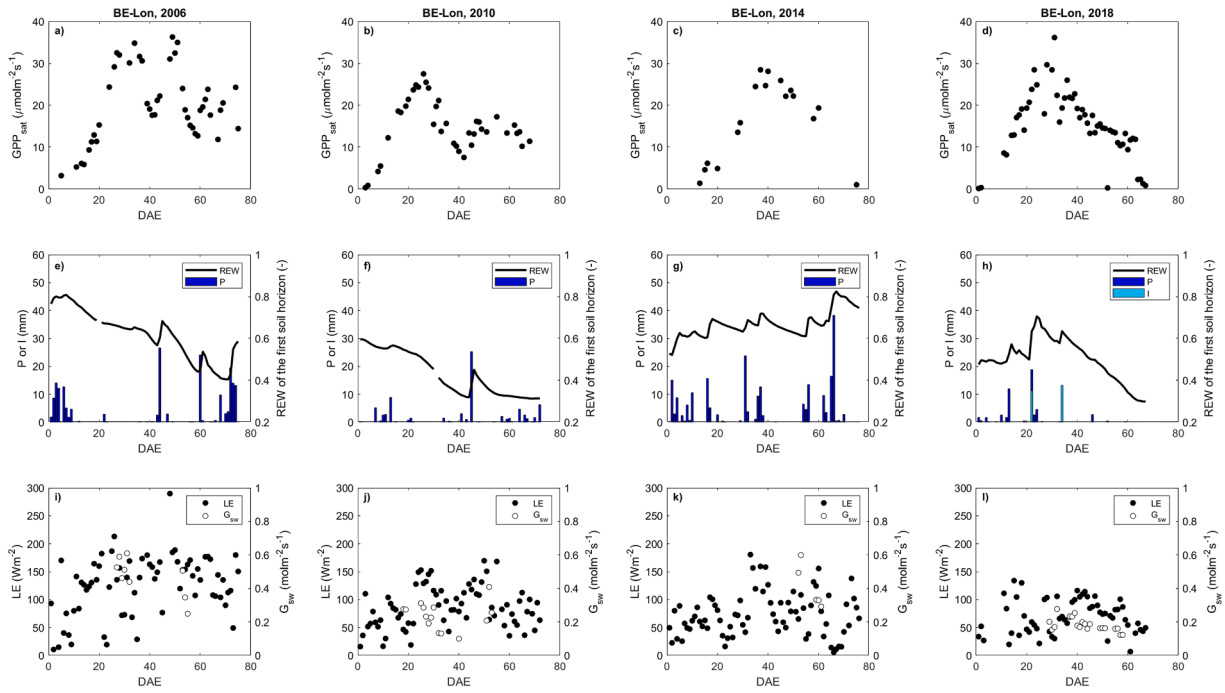

Fig. 2. Gross primary production under high irradiance (GPP_{sat}; subplots a to d), relative extractable water (*REW*; subplots e to h), latent heat flux (*LE*) and canopy conductance to water vapor (G_{sw}; subplots i to f) daily means. Daily sums of precipitation (P) and irrigation (I) are displayed on the second line (subplots e to h). DAE corresponds to days after emergence.

Table 3
Statistical proprieties of the regressions: REW breakpoint, asymptote (or averaged value), slope, model p-value ($pval_{mod}$) and R^2 for $V_{cmax,app,25}$, G_1, sensitivity analysis on $V_{cmax,app,25}$ and for *DWCI*. Parameters are given with their standard deviation. For the p-values, *** : <0.001, ** : <0.01, *: <0.05, ns : >0.05.

	$V_{cmax,app,25}$					G_1				
	REW breakpoint (-)	Asymptote ($V_{cmax,app,25}$*) or averaged value (μmol m^{-2} s^{-1})	Slope (μmol m^{-2} s^{-1})	$pval_{mod}$ (-)	R^2 (-)	REW breakpoint (-)	Asymptote (G_1*) or averaged value ($kPa^{0.5}$)	Slope ($kPa^{0.5}$)	$pval_{mod}$ (-)	R^2 (-)
2006	0.58 ± 0.01 ***	121 ± 2.93 ***	704 ± 94.1 ***	< 0.001	0.82	/	4.35 ± 0.80	/	/	/
2010	0.45 ± 0.02 ***	128 ± 6.11 ***	821 ± 137 **	< 0.001	0.69	0.44 ± 0.05 ***	1.69 ± 0.24 ***	−12.7 ± 5.63*	< 0.01	0.21
2014	/	80.2 ± 5.25	/	/	/	/	4.44 ± 1.45	/	/	/
2018	0.51 ± 0.01 ***	98.7 ± 1.69 ***	324 ± 36.2 ***	< 0.001	0.44	0.45 ± 0.03 ***	2.37 ± 0.05***	−7.27 ± 3.41*	< 0.05	0.09

	Sensitivity analysis on $V_{cmax,app,25}$				
	REW breakpoint (-)	Asymptote (-)	Slope (-)	$pval_{mod}$ (-)	R^2 (-)
2006, 2010, 2018	0.46 ± 0.01 ***	1.08 ± 0.02 ***	−11.8 ± 1.31 ***	< 0.001	0.55
	DWCI				
	REW breakpoint (-)	Asymptote (-)	Slope (-)	$pval_{mod}$ (-)	R^2 (-)
2006, 2010, 2018	0.45 ± 0.04 ***	0.91 ± 0.01 ***	2.04± 0.95 **	< 0.01	0.41

(Fig. 4). The *REW* breakpoint of the sensitivity analysis characterizes a tipping point illustrating the importance of including NSOL of GPP for potatoes during edaphic drought.

3.2.4. Coupling between carbon and water fluxes

In 2010 and 2018, NSOL induced a decoupling between $GPP\sqrt{VPD_s}$ and *LE*, characterized by a shift of the $GPP\sqrt{VPD_s}$ maximum toward morning hours (Fig. 5).

During these years, a clear change in the $GPP\sqrt{VPD_s}$ dynamics was observed, with a maximum value being reached in the early morning (Fig. 6). This decoupling between carbon and water fluxes was not observed in 2006 and 2014, which can be explained by favorable weather conditions in 2014 (absence of water stress) and probably the relatively low intensity of the drought effect on $V_{cmax,app,25}$ in 2006 ($V_{cmax,app,25}$ remained higher than 50 μmol m^{-2} s^{-1}). *DWCI* decreased when *REW* passed below a threshold of 0.45 ± 0.04 (Fig. 6) which was similar to the thresholds for the $GPP_{Vcmax,app,25}{}^{*}/GPP_{sat}$ ratio and $V_{cmax,app,25}$ dependence on REW (Table 3).

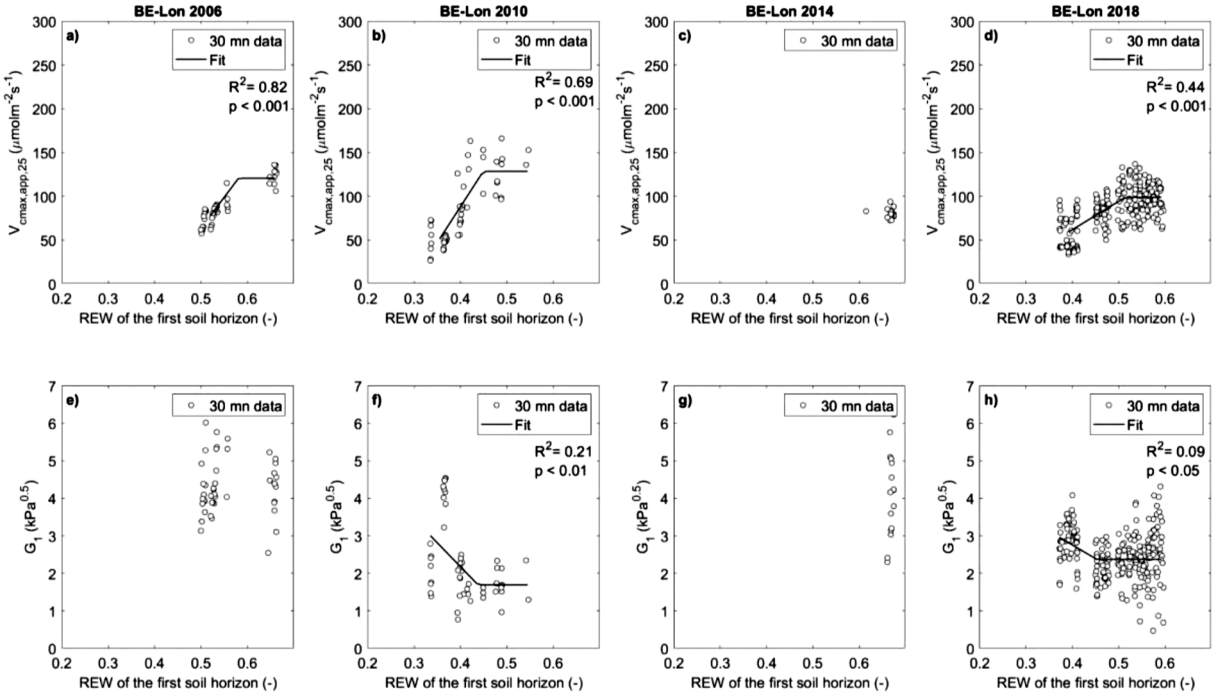

Fig. 3. Apparent maximum carboxylation rate at 25 °C ($V_{cmax,app,25}$; subplots a to d) and slope parameter of the USO model (G_1; subplots e to h) dynamics in function of the relative extractable water (*REW*) for the years studied. p refers to the p-value comparing the segmented model to a linear model (p-val_{mod} in Table 3).

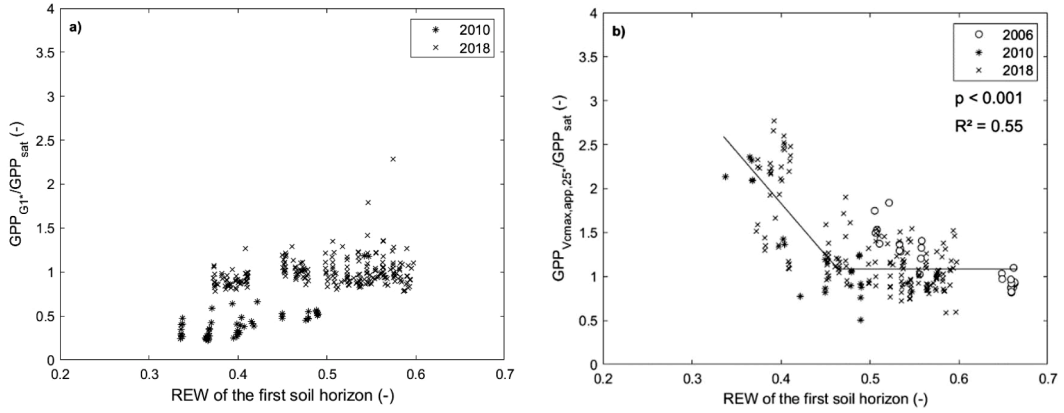

Fig. 4. Sensitivity analysis for the modeling of GPP by setting $V_{cmax,app,25}$ and G_1 to a constant value when *REW* is non limiting(respectively $GPP_{Vcmax,app,25}{}^*$ and $GPP_{G1}{}^*$). The ratios $GPP_{G1}{}^*/GPP_{sat}$ (subplot a) and $GPP_{Vcmax,app,25}{}^*/GPP_{sat}$ (subplot b) were only calculated for the years when a decrease in $V_{cmax,app,25}$ and/or an increase in G_1 were observed. p refers to the p-value comparing the segmented model to a linear model (p-val_{mod} in Table 3).

4. Discussion

4.1. Photosynthesis limitations and methodological considerations

Whatever the year analyzed, we found a global pattern of reduction of photosynthesis capacities due to the influence of soil water availability. Only $V_{cmax,app,25}$ decreased with *REW*, which suggests that the β stress function should only be applied when *REW* passes below the breakpoint of 0.46 ± 0.01 (for the varieties of potatoes cultivated at BE-Lon and the soil type present on this site). Not implementing water stress effect on $V_{cmax,app,25}$ would significantly overestimate GPP. This provides strong evidence that NSOL played a major role (or even unique because SOL has not been observed) in carbon assimilation dynamics of potato under high irradiance and during edaphic drought during the four years studied. Moreover, our study was performed at the canopy level which is representative of the physiological reaction of the entire ecosystem to drought since the "big-leaf" approach includes all the leaves within the footprint of the EC tower. These conclusions are in accordance with previous studies carried out on forests (Gourlez de la Motte et al., 2020) and on various non-cropland ecosystems (Chen et al., 2019), tending to show that NSOL should not be neglected for many plant functional types. At the leaf-level, numerous studies have evaluated the importance of NSOL on photosynthesis using coupled gas-exchange and fluorescence measurements for various crop (Flexas et al., 2008; Wang et al., 2018) and tree species (Grassi et Magnani, 2005; Perez-Martin et al., 2014; Zait et Schwartz, 2018; Zhu et al., 2021). While most of the studies conducted on potato aimed at identifying the physiological response to imposed drought through the dynamics of photosynthetic capacities or stomatal closure (Ramírez et al., 2016; Li et al., 2017; Boguszewska-Mańkowska et al., 2018; Silva-Diàz et al., 2020; Aliche et al., 2020), the calibration of the β stress function during edaphic water stress for this crop is lacking. Our study provides a function of *REW* that can be

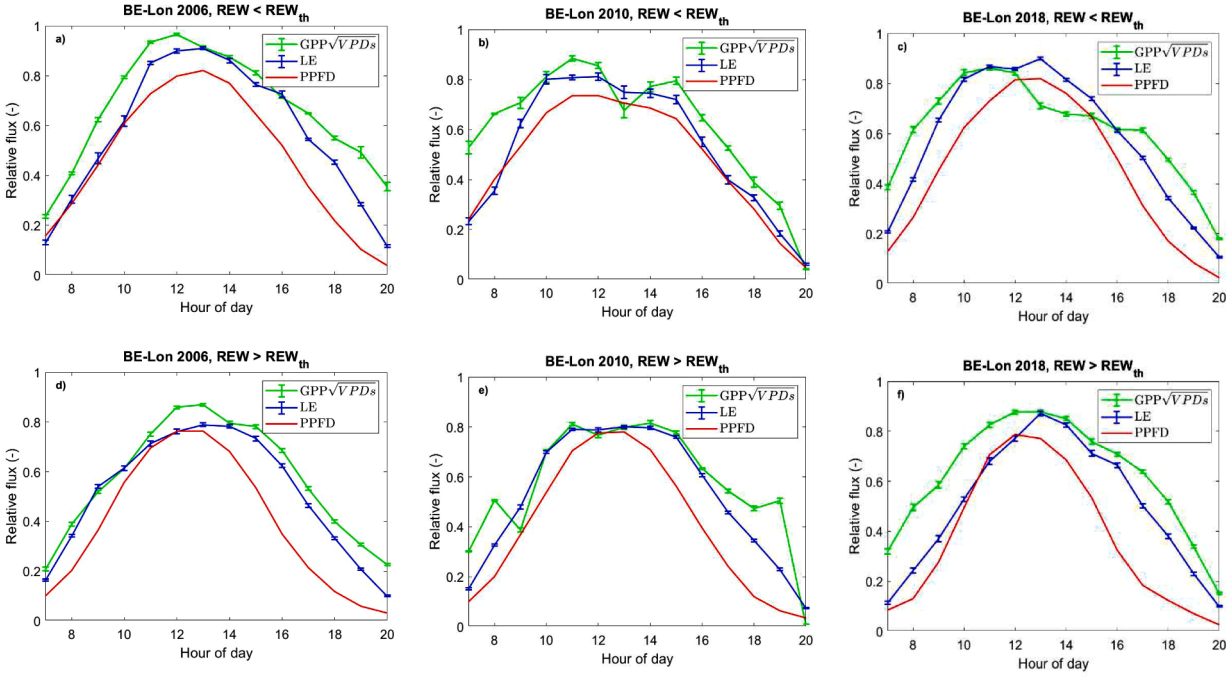

Fig. 5. Latent heat flux (LE), photosynthetic photon flux density (PPFD) and normalized GPP ($GPP\sqrt{VPD_s}$) hourly means and standard deviation when relative extractable water (*REW*) is lower than *REW* breakpoints of segmented linear regressions for $V_{cmax,app,25}$ (REW_{th} - subplots a to c) or when *REW* is not limiting (subplots d to f) for the three years when non-stomatal limitations were observed (Table 3).

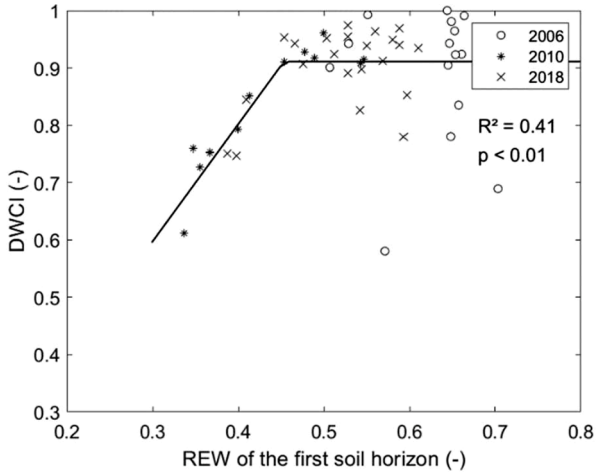

Fig. 6. Diurnal water carbon index (*DWCI*) daily dynamics in function of the relative extractable water (*REW*). p refers to the p-value comparing the segmented model to a linear model ($p\text{-}val_{mod}$ in Table 3).

directly translated to models of photosynthesis in LSMs.

The decrease in $V_{cmax,app,25}$ illustrates an alteration of the photosynthesis capacities of the crop, either by a restriction of CO_2 diffusion through the mesophyll, real biochemical alteration of the photosynthetic apparatus, or both. Excessive diffusive limitation of CO_2 by the mesophyll may lead to an accumulation of ATP and NADPH which can no longer used by the Calvin cycle, causing energy imbalance, oxidative stress and damage to cell components (Pinheiro and Chaves, 2011). Moreover, biochemical alteration of photosynthetic capacities can be caused by photo-inhibition and/or irreversible inactivation of PSII, as has been identified during prolonged water stress (Obidiegwu, 2015). Our study did not allow the identification of the NSOL causes as techniques used to quantify mesophyll conductance (involving carbon isotopes or fluorescence) were not tested. No global application of a model representing these processes has yet emerged since its implementation would require a heavy calibration for all plant functional types, a procedure that has not yet been achieved. Future studies should focus on continuous measurements of water extraction, photosynthetic capacities, mesophyll and stomatal conductance during dry periods and subsequent recovery episodes, so drought impacts on ecosystems can be fully understood and mechanistically modeled (Flexas et al., 2018).

The relatively similar *REW* breakpoints for all growing seasons suggests that the same amount of water in the root zone was required to ensure that saturated photosynthesis remained unaffected by drought, whatever the timing of drought appearance or the potato varieties. This also indicates that the water needs for potato crops were similar during the vegetative (2006) or reproductive (2010, 2018) stages. This observation coincides with early studies stating that "soil moisture should never be allowed to drop below 50 % of the available range of moisture" for potato crop (Singh, 1969), confirming that potato is sensitive to water stress. Models such as Aquacrop usually calibrate similar functions of *REW* to simulate drought stress on crop physiology with upper thresholds of 0.6 for canopy expansion, 0.7 for canopy senescence, or 0.55 for stomatal control (Raes et al., 2018). The degree of calibration of these thresholds is defined as minimum and requires further investigations for potatoes (Montoya et al., 2016; Raes et al., 2018). The *REW* breakpoint of 0.46 proposed by this study could be used to design irrigation management strategies from SWC measurements in surface soil layers to avoid the risk of crop abiotic damage. This information is complementary to high-throughput phenotyping techniques (Musse et al., 2021) for selecting drought-tolerant varieties from the criteria of the lowest *REW* threshold for maintaining an optimum photosynthetic rate. The generalization of our results could be enhanced by applying the procedure and analysis proposed in this paper on other crop sites of the ICOS network where potato was cultivated, which could provide complementary *REW* thresholds for other soil types.

The method used for calculating *REW* considers that all the roots have the same ability to extract water from the first soil horizon, whatever their age, diameter, architecture, location, or function. This assumption can be challenged, as it has been shown that the root water

uptake can be dependent on root density, morphology, and physiology (Kumar et al., 2015). For example, Stalham and Allen (2004) showed that 5 % of the deepest roots can account for a half of the total water uptake for the potato cultivar Cara. Some models do consider these dependences but are difficult to implement at a plot scale due to the high number of inputs and parameters required. Nonetheless, *REW* remains a useful indicator to determine the amount of available water in the soil from soil hydraulic or granulometric properties that are available for all the ICOS sites.

Some bias in the results can originate from errors in the estimation of C_i (Eq. (12)), and in the calculation of G_{sw} by Eq. (7). The Penman-Monteith equation assumes that the minimal gas diffusion through stomatal apertures (G_0) is set to zero and that no transfer through the cuticle (in parallel with diffusion through stomata) is considered. However, as the cuticle may represent the main pathway for transpiration during drought (Boyer, 2015; Duursma et al., 2019), these assumptions could possibly lead to an underestimation of G_{sw} and then C_i by Eq. (12) (Boyer, 2015). To counter this potential drawback, C_i could be directly measured at the leaf level by a gas exchange chamber (Boyer, 2015), or the computation of G_{sw} could be modified by considering G_0 determined from laboratory measurements (Wang et al., 2018). However, estimating G_0 by data adjustment on the USO model remains challenging due to statistical considerations (Duursma et al., 2019), which explains that G_0 is often set to zero or to a constant value in coupled photosynthesis-stomata conductance models (Medlyn et al., 2017; Duursma et al., 2019).

4.2. Stomatal conductance modeling during drought

While the empirical Ball-Berry (Ball et al., 1987) stomatal conductance model has been used as a baseline in climate models since the mid-1990s (Bonan et al., 2014), many LSMs currently use the USO model (Eq. (13)) to estimate G_{sw} (Kala et al., 2015; Lawrence et al., 2019). However, the calibration of the response of G_1 to edaphic water stress remains a key element for improving model predictions in a climate change context. Although most models downregulate G_1 with soil moisture (following the stomatal optimality theory; Mäkelä, 1996), numerous studies have observed a different G_1 dependance to soil moisture using leaf-level or ecosystem fluxes data (Zhou et al., 2013; Chen et al., 2019; Gourlez de la Motte et al., 2020). In line with these studies, our results showed that G_1 remained constant (or even increased) with the decrease in *REW* for potato. This observation suggests the absence of regulation of stomata opening during drought and indicates a deviation from the optimality theory as the increase of G_1 for low *REW* corresponds to a rise of the water cost of carbon gain. This behavior can be explained by a decrease of $V_{cmax,app,25}$ (inducing a decline of the carbon gain through the alteration of efficiency of RuBisCO to fix CO_2 in the Calvin cycle) more important than the corresponding increase in the water transport capacity. This hypothesis is supported by Aliche et al. (2020), who observed an adaptation of the hydraulic architecture of four potato cultivars in response to dehydration through and an increase in xylem flux density and an increase in the ratio between small and large xylem vessels, preventing from cavitation and facilitating the transport of water and assimilates.

When $V_{cmax,app,25}$ was relatively low, NSOL induced a reduction of GPP_{sat} leading to a decrease of the G_{sw} computed by Eq. (13), but partly compensated by an increase of G_1. This may explain the decoupling between $GPP\sqrt{VPD_s}$ and *LE* intra-day dynamics with decreasing *REW* and emergence of NSOL which induced an inhibition of photosynthetic capacities independently from transpiration. Similar results were presented by Nelson et al. (2018), who reported a decrease of *DWCI* during the 2003 drought in Puéchabon and for dry savanna/grassland plant functional types during dry episodes.

5. Conclusion

In this study, a "big-leaf" approach including the FvCB model for photosynthesis and the USO model for stomatal conductance was used to infer the physiological properties of a potato crop for four consecutive growing seasons at the ICOS site of Lonzée in Belgium. Drought induced a decrease in $V_{cmax,app,25}$ with similar *REW* breakpoints and unstressed values for all years, which highlighted a uniform pattern of drought effects on GPP. A global value of 46 % of available soil water was obtained from a sensitivity analysis, which highlights the importance of implementing *REW* effects on $V_{cmax,app,25}$ to reproduce drought effects on GPP. The coupling of this representation with a constant value or a linear increase with *REW* of the slope parameter (G_1) in USO model was sufficient to simultaneously reproduce both carbon and water flux dynamics at seasonal and diurnal scales during drying-up episodes. The inclusion of the effects of drought on NSOL in LSMs for potatoes is recommended to properly implement the effects of drought on water and carbon cycles.

CRediT authorship contribution statement

Quentin Beauclaire: Conceptualization, Formal analysis, Software, Writing – original draft, Writing – review & editing, Validation. **Bernard Heinesch:** Resources, Writing – review & editing. **Bernard Longdoz:** Resources, Validation, Supervision, Writing – review & editing.

Declaration of Competing Interest

The authors declare that they have no known competing financial interests or personal relationships that could have appeared to influence the work reported in this paper.

Data availability

Data will be made available on request.

Acknowledgments and funding

This research was conducted within the framework of the ICOS Wallonia project, which is supported by the Service Public de Wallonie, Belgium [1217769]. The researchers were funded by the Federation Wallonie Bruxelles (FWB).

Supplementary materials

Supplementary material associated with this article can be found, in the online version, at doi:10.1016/j.agrformet.2023.109782.

References

Aliche, E.B., Prusova-Bourke, A., Ruiz-Sanchez, M., Oortwijn, M., Gerkema, E., Van As, H., Visser, R.G.F., van der Linden, C.G., 2020. Morphological and physiological responses of the potato stem transport tissues to dehydration stress. Planta 251, 45. https://doi.org/10.1007/s00425-019-03336-7.

Allen, R.G., 1998. Food and agriculture organization of the United Nations (Eds.). Crop evapotranspiration: Guidelines for Computing Crop Water Requirements. FAO irrigation and drainage paper. Food and Agriculture Organization of the United Nations, Rome.

Aubinet, M., Moureaux, C., Bodson, B., Dufranne, D., Heinesch, B., Suleau, M., Vancutsem, F., Vilret, A., 2009. Carbon sequestration by a crop over a 4-year sugar beet/winter wheat/seed potato/winter wheat rotation cycle. Agric. For. Meteorol. 149, 407–418. https://doi.org/10.1016/j.agrformet.2008.09.003.

Aubinet, M., Vesala, T., Papale, D., 2012. Eddy Covariance: A Practical Guide to Measurement and Data Analysis. Springer Netherlands, Dordrecht. https://doi.org/10.1007/978-94-007-2351-1.

Ball, J.T., Woodrow, I.E., Berry, J.A., 1987. A model predicting stomatal conductance and its contribution to the control of photosynthesis under different environmental conditions. In: Biggins, J. (Ed.), Progress in Photosynthesis Research: Volume 4 Proceedings of the VIIth International Congress on Photosynthesis Providence.

Rhode Island, USA. Springer Netherlands, Dordrecht, pp. 221–224. https://doi.org/10.1007/978-94-017-0519-6_48. August 10–15, 1986.
Bernacchi, C.J., Singsaas, E.L., Pimentel, C., Portis Jr., A.R., Long, S.P., 2001. Improved temperature response functions for models of Rubisco-limited photosynthesis: *In vivo* Rubisco enzyme kinetics. Plant Cell Environ. 24, 253–259. https://doi.org/10.1111/j.1365-3040.2001.00668.x.
Boguszewska-Mańkowska, D., Pieczyński, M., Wyrzykowska, A., Kalaji, H.M., Sieczko, L., Szweykowska-Kulińska, Z., Zagdańska, B., 2018. Divergent strategies displayed by potato (Solanum tuberosum L.) cultivars to cope with soil drought. J. Agron. Crop Sci. 204, 13–30. https://doi.org/10.1111/jac.12245.
Bonan, G.B., Williams, M., Fisher, R.A., Oleson, K.W., 2014. Modeling stomatal conductance in the earth system: linking leaf water-use efficiency and water transport along the soil–plant–atmosphere continuum. Geosci. Model Dev. 7, 2193–2222. https://doi.org/10.5194/gmd-7-2193-2014.
Boyer, J.S., 2015. Impact of cuticle on calculations of the CO2 concentration inside leaves. Planta 242, 1405–1412. https://doi.org/10.1007/s00425-015-2378-1.
Breda, N.J.J., 2003. Ground-based measurements of leaf area index: a review of methods, instruments and current controversies. J. Exp. Bot. 54, 2403–2417. https://doi.org/10.1093/jxb/erg263.
Buysse, P., Bodson, B., Debacq, A., De Ligne, A., Heinesch, B., Manise, T., Moureaux, C., Aubinet, M., 2017. Carbon budget measurement over 12 years at a crop production site in the silty-loam region in Belgium. Agric. For. Meteorol. 246, 241–255. https://doi.org/10.1016/j.agrformet.2017.07.004.
Chen, B., Chen, J.M., Baldocchi, D.D., Liu, Y., Wang, S., Zheng, T., Black, T.A., Croft, H., 2019. Including soil water stress in process-based ecosystem models by scaling down maximum carboxylation rate using accumulated soil water deficit. Agric. For. Meteorol. 276–277, 107649 https://doi.org/10.1016/j.agrformet.2019.107649.
Chiang, F., Mazdiyasni, O., AghaKouchak, A., 2021. Evidence of anthropogenic impacts on global drought frequency, duration, and intensity. Nat. Commun. 12, 2754. https://doi.org/10.1038/s41467-021-22314-w.
Cowan, I., Farquhar, G., 1977. Stomatal function in relation to leaf metabolism and environment. Symp. Soc. Exp. Biol. 31, 471—505.
Damour, G., Simonneau, T., Cochard, H., Urban, L., 2010. An overview of models of stomatal conductance at the leaf level: models of stomatal conductance. Plant Cell Environ. https://doi.org/10.1111/j.1365-3040.2010.02181.x no-no.
Duursma, R.A., Blackman, C.J., Lopéz, R., Martin-StPaul, N.K., Cochard, H., Medlyn, B. E., 2019. On the minimum leaf conductance: its role in models of plant water use, and ecological and environmental controls. New Phytol. 221, 693–705. https://doi.org/10.1111/nph.15395.
Egea, G., Verhoef, A., Vidale, P.L., 2011. Towards an improved and more flexible representation of water stress in coupled photosynthesis–stomatal conductance models. Agric. For. Meteorol. 151, 1370–1384. https://doi.org/10.1016/j.agrformet.2011.05.019.
Fahad, S., Bajwa, A.A., Nazir, U., Anjum, S.A., Farooq, A., Zohaib, A., Sadia, S., Nasim, W., Adkins, S., Saud, S., Ihsan, M.Z., Alharby, H., Wu, C., Wang, D., Huang, J., 2017. Crop production under drought and heat stress: plant responses and management options. Front. Plant Sci. 8, 1147. https://doi.org/10.3389/fpls.2017.01147.
Farquhar, G.D., Sharkey, T.D., 1982. Stomatal conductance and photosynthesis. Annu. Rev. Plant. Physiol. 33, 317–345. https://doi.org/10.1146/annurev.pp.33.060182.001533.
Farquhar, G.D., von Caemmerer, S., Berry, J.A., 1980. A biochemical model of photosynthetic CO_2 assimilation in leaves of C_3 species. Planta 149, 78–90. https://doi.org/10.1007/BF00386231.
Flexas, J., Bota, J., Loreto, F., Cornic, G., Sharkey, T.D., 2004. Diffusive and metabolic limitations to photosynthesis under drought and salinity in C_3 plants. Plant Biol. 6, 269–279. https://doi.org/10.1055/s-2004-820867.
Flexas, J., Carriquí, M., Nadal, M., 2018. Gas exchange and hydraulics during drought in crops: who drives whom? J. Exp. Bot. 69, 3791–3795. https://doi.org/10.1093/jxb/ery235.
Flexas, J., Ribas-Carbó, M., Diaz-Espejo, A., Galmés, J., Medrano, H., 2008. Mesophyll conductance to CO_2 : current knowledge and future prospects. Plant Cell Environ. 31, 602–621. https://doi.org/10.1111/j.1365-3040.2007.01757.x.
Food and Agriculture Organization of the United Nations, 2021. FAOSTAT Database. Rome, Italy: FAO. Retrieved May 30, 2021 from. http://www.fao.org/faostat/en/#data.
Franz, D., Acosta, M., Altimir, N., Arriga, N., Arrouays, D., Aubinet, M., Aurela, M., Ayres, E., López-Ballesteros, A., Barbaste, M., Berveiller, D., Biraud, S., Boukir, H., Brown, T., Brümmer, C., Buchmann, N., Burba, G., Carrara, A., Cescatti, A., Ceschia, E., Clement, R., Cremonese, E., Crill, P., Darenova, E., Dengel, S., D'Odorico, P., Filippa, G., Fleck, S., Fratini, G., Fuß, R., Gielen, B., Gogo, S., Grace, J., Graf, A., Grelle, A., Gross, P., Grünwald, T., Haapanala, S., Hehn, M., Heinesch, B., Heiskanen, J., Herbst, M., Herschlein, C., Hörtnagl, L., Hufkens, K., Ibrom, A., Jolivet, C., Joly, L., Jones, M., Kiese, R., Klemedtsson, L., Kljun, N., Klumpp, K., Kolari, P., Kolle, O., Kowalski, A., Kutsch, W., Laurila, T., de Ligne, A., Linder, S., Lindroth, A., Lohila, A., Longdoz, B., Mammarella, I., Manise, T., Jiménez, S.M., Matteucci, G., Mauder, M., Meier, P., Merbold, L., Mereu, S., Metzger, S., Migliavacca, M., Mölder, M., Montagnani, L., Moureaux, C., Nelson, D., Nemitz, E., Nicolini, G., Nilsson, M.B., de Beeck, M.O., Osborne, B., Löfvenius, M.O., Pavelka, M., Peichl, M., Peltola, O., Pihlatie, M., Pitacco, A., Pokorný, R., Pumpanen, J., Ratié, C., Rebmann, C., Roland, M., Sabbatini, S., Saby, N.P.A., Saunders, M., Schmid, H.P., Schrumpf, M., Sedlák, P., Ortiz, P.S., Siebicke, L., Šigut, L., Silvennoinen, H., Simioni, G., Skiba, U., Sonnentag, O., Soudani, K., Soulé, P., Steinbrecher, R., Tallec, T., Thimonier, A., Tuittila, E.-S., Tuovinen, J.-P., Vestin, P., Vincent, G., Vincke, C., Vitale, D., Waldner, P., Weslien, P., Wingate, L., Wohlfahrt, G., Zahniser, M., Vesala, T., 2018. Towards long-term standardised carbon and greenhouse gas observations for monitoring Europe's terrestrial ecosystems: a review. Int. Agrophys. 32, 439–455. https://doi.org/10.1515/intag-2017-0039.
Goffart, J.-P., Haverkort, A., Storey, M., Haase, N., Martin, M., Lebrun, P., Ryckmans, D., Florins, D., Demeulemeester, K., 2022. Potato Production in Northwestern Europe (Germany, France, the Netherlands, United Kingdom, Belgium): Characteristics. Challenges and Opportunities. Potato Res. https://doi.org/10.1007/s11540-021-09535-8. Issues.
Gourlez de la Motte, L., Beauclaire, Q., Heinesch, B., Cuntz, M., Foltýnová, L., Sigut, L., Kowalska, N., Manca, G., Ballarin, I., Vincke, C., Roland, M., Ibrom, A., Lousteau, D., Siebicke, L., Bernard, L., 2020. Non-stomatal Processes Reduce Gross Primary Productivity in Temperate Forest Ecosystems During Severe Edaphic Drought. Philosophical Transactions of The Royal Society B Biological Sciences In Press. https://doi.org/10.1098/RSTB-2019-0527.
Granier, A., Bréda, N., Biron, P., Villette, S., 1999. A lumped water balance model to evaluate duration and intensity of drought constraints in forest stands. Ecolog. Model. 116, 269–283. https://doi.org/10.1016/S0304-3800(98)00205-1.
Grassi, G., Magnani, F., 2005. Stomatal, mesophyll conductance and biochemical limitations to photosynthesis as affected by drought and leaf ontogeny in ash and oak trees. Plant Cell Environ. 28, 834–849. https://doi.org/10.1111/j.1365-3040.2005.01333.x.
Harper, A.B., Williams, K.E., McGuire, P.C., Duran Rojas, M.C., Hemming, D., Verhoef, A., Huntingford, C., Rowland, L., Marthews, T., Breder Eller, C., Mathison, C., Nobrega, R.L.B., Gedney, N., Vidale, P.L., Otu-Larbi, F., Pandey, D., Garrigues, S., Wright, A., Slevin, D., De Kauwe, M.G., Blyth, E., Ardö, J., Black, A., Bonal, D., Buchmann, N., Burban, B., Fuchs, K., de Grandcourt, A., Mammarella, I., Merbold, L., Montagnani, L., Nouvellon, Y., Restrepo-Coupe, N., Wohlfahrt, G., 2021. Improvement of modeling plant responses to low soil moisture in JULESvn4.9 and evaluation against flux tower measurements. Geosci. Model Dev. 14, 3269–3294. https://doi.org/10.5194/gmd-14-3269-2021.
Heinesch, B., De Ligne, A., Manise, T., Longdoz, B., ICOS Ecosystem Thematic Centre, 2022. Warm Winter 2020 Ecosystem Eddy Covariance Flux Product from Lonzee (Version 1.0) [Data Set]. ICOS Carbon Portal. https://doi.org/10.18160/46P3-WT1D.
Hetherington, A.M., Woodward, F.I., 2003. The role of stomata in sensing and driving environmental change. Nature 424, 901–908. https://doi.org/10.1038/nature01843.
Kala, J., De Kauwe, M.G., Pitman, A.J., Lorenz, R., Medlyn, B.E., Wang, Y.-P., Lin, Y.-S., Abramowitz, G., 2015. Implementation of an optimal stomatal conductance scheme in the Australian Community Climate Earth Systems Simulator (ACCESS1.3b). Geosci. Model Dev. 8, 3877–3889. https://doi.org/10.5194/gmd-8-3877-2015.
Knauer, J., El-Madany, T.S., Zaehle, S., Migliavacca, M., 2018a. Bigleaf—an R package for the calculation of physical and physiological ecosystem properties from eddy covariance data. PLoS One 13, e0201114. https://doi.org/10.1371/journal.pone.0201114.
Knauer, J., Zaehle, S., Medlyn, B.E., Reichstein, M., Williams, C.A., Migliavacca, M., De Kauwe, M.G., Werner, C., Keitel, C., Kolari, P., Limousin, J., Linderson, M., 2018b. Towards physiologically meaningful water-use efficiency estimates from eddy covariance data. Glob. Chang. Biol. 24, 694–710. https://doi.org/10.1111/gcb.13893.
Krich, C., Mahecha, M.D., Migliavacca, M., De Kauwe, M.G., Griebel, A., Runge, J., Miralles, D.G., 2022. Decoupling between ecosystem photosynthesis and transpiration: a last resort against overheating. Environ. Res. Lett. 17, 044013 https://doi.org/10.1088/1748-9326/ac583e.
Kumar, R., Shankar, V., Jat, M.K., 2015. Evaluation of root water uptake models – a review. ISH J. Hydraul. Eng. 21, 115–124. https://doi.org/10.1080/09715010.2014.981955.
Lawrence, D.M., Fisher, R.A., Koven, C.D., Oleson, K.W., Swenson, S.C., Bonan, G., Collier, N., Ghimire, B., Van Kampenhout, L., Kennedy, D., Kluzek, E., Lawrence, P. J., Li, F., Li, H., Lombardozzi, D., Riley, W.J., Sacks, W.J., Shi, M., Vertenstein, M., Wieder, W.R., Xu, C., Ali, A.A., Badger, A.M., Bisht, G., Van Den Broeke, M., Brunke, M.A., Burns, S.P., Buzan, J., Clark, M., Craig, A., Dahlin, K., Drewniak, B., Fisher, J.B., Flanner, M., Fox, A.M., Gentine, P., Hoffman, F., Keppel-Aleks, G., Knox, R., Kumar, S., Lenaerts, J., Leung, L.R., Lipscomb, W.H., Lu, Y., Pandey, A., Pelletier, J.D., Perket, J., Randerson, J.T., Ricciuto, D.M., Sanderson, B.M., Slater, A., Subin, Z.M., Tang, J., Thomas, R.Q., Val Martin, M., Zeng, X., 2019. The community land model version 5: description of new features, benchmarking, and impact of forcing uncertainty. J. Adv. Model. Earth Syst. 11, 4245–4287. https://doi.org/10.1029/2018MS001583.
Li, J., Cang, Z., Jiao, F., Bai, X., Zhang, D., Zhai, R., 2017. Influence of drought stress on photosynthetic characteristics and protective enzymes of potato at seedling stage. J. Saud. Soc. Agricult. Sci. 16, 82–88. https://doi.org/10.1016/j.jssas.2015.03.001.
Li, Q., Serbin, S.P., Lamour, J., Davidson, K.J., Ely, K.S., Rogers, A., 2022. Implementation and evaluation of the unified stomatal optimization approach in the functionally assembled terrestrial ecosystem simulator (FATES) (preprint). Biogeosciences. https://doi.org/10.5194/gmd-2021-414.
Lutaladio, N., Castaldi, L., 2009. Potato: the hidden treasure. J. Food Compos. Anal. 22, 491–493. https://doi.org/10.1016/j.jfca.2009.05.002.
Mäkelä, A., 1996. Optimal control of gas exchange during drought: theoretical analysis. Ann. Bot. 77, 461–468. https://doi.org/10.1006/anbo.1996.0056.
Marchin, R.M., Backes, D., Ossola, A., Leishman, M.R., Tjoelker, M.G., Ellsworth, D.S., 2022. Extreme heat increases stomatal conductance and drought-induced mortality risk in vulnerable plant species. Glob. Chang. Biol. 28, 1133–1146. https://doi.org/10.1111/gcb.15976.
Mcmaster, G., 1997. Growing degree-days: one equation, two interpretations. Agric. For. Meteorol. 87, 291–300. https://doi.org/10.1016/S0168-1923(97)00027-0.

Medlyn, B.E., De Kauwe, M.G., Lin, Y.-S., Knauer, J., Duursma, R.A., Williams, C.A., Arneth, A., Clement, R., Isaac, P., Limousin, J.-M., Linderson, M.-L., Meir, P., Martin-StPaul, N., Wingate, L., 2017. How do leaf and ecosystem measures of water-use efficiency compare? New Phytol. 216, 758–770. https://doi.org/10.1111/nph.14626.

Medlyn, B.E., Dreyer, E., Ellsworth, D., Forstreuter, M., Harley, P.C., Kirschbaum, M.U.F., Le Roux, X., Montpied, P., Strassemeyer, J., Walcroft, A., Wang, K., Loustau, D., 2002. Temperature response of parameters of a biochemically based model of photosynthesis. II. A review of experimental data: temperature response of photosynthetic parameters - review. Plant Cell Environ. 25, 1167–1179. https://doi.org/10.1046/j.1365-3040.2002.00891.x.

Medlyn, B.E., Duursma, R.A., Eamus, D., Ellsworth, D.S., Prentice, I.C., Barton, C.V.M., Crous, K.Y., De Angelis, P., Freeman, M., Wingate, L., 2011. Reconciling the optimal and empirical approaches to modeling stomatal conductance: reconciling optimal and empirical stomatal models. Glob. Chang. Biol. 17, 2134–2144. https://doi.org/10.1111/j.1365-2486.2010.02375.x.

Monteith, J.L., 1965. Evaporation and environment. Symp. Soc. Exp. Biol. 19, 205–234.

Montoya, F., Camargo, D., Ortega, J.F., Córcoles, J.I., Domínguez, A., 2016. Evaluation of Aquacrop model for a potato crop under different irrigation conditions. Agric. Water Manage. 164, 267–280. https://doi.org/10.1016/j.agwat.2015.10.019.

Musse, M., Hajjar, G., Ali, N., Billiot, B., Joly, G., Pépin, J., Quellec, S., Challois, S., Mariette, F., Cambert, M., Fontaine, C., Ngo-Dinh, C., Jamois, F., Barbary, A., Leconte, P., Deleu, C., Leport, L., 2021. A global non-invasive methodology for the phenotyping of potato under water deficit conditions using imaging, physiological and molecular tools. Plant Method. 17, 81. https://doi.org/10.1186/s13007-021-00771-0.

Nelson, J.A., Carvalhais, N., Migliavacca, M., Reichstein, M., Jung, M., 2018. Water-stress-induced breakdown of carbon–water relations: indicators from diurnal FLUXNET patterns. Biogeosciences 15, 2433–2447. https://doi.org/10.5194/bg-15-2433-2018.

Obidiegwu, J.E., 2015. Coping with drought: stress and adaptive responses in potato and perspectives for improvement. Front. Plant Sci. 6 https://doi.org/10.3389/fpls.2015.00542.

Oliver, R.J., Mercado, L.M., Clark, D.B., Huntingford, C., Taylor, C.M., Vidale, P.L., McGuire, P.C., Todt, M., Folwell, S., Shamsudheen Semeena, V., Medlyn, B.E., 2022. Improved representation of plant physiology in the JULES-vn5.6 land surface model: photosynthesis, stomatal conductance and thermal acclimation. Geosci. Model Dev. 15, 5567–5592. https://doi.org/10.5194/gmd-15-5567-2022.

Pastorello, G., Trotta, C., Canfora, E., Chu, H., Christianson, D., Cheah, Y.-W., Poindexter, C., Chen, J., Elbashandy, A., Humphrey, M., Isaac, P., Polidori, D., Ribeca, A., Ingen, C., Zhang, L., Amiro, B., Ammann, C., Arain, M., Ardö, J., Papale, D., 2020. The FLUXNET2015 dataset and the ONEFlux processing pipeline for eddy covariance data. Sci. Data 7. https://doi.org/10.1038/s41597-020-0534-3.

Perez-Martin, A., Michelazzo, C., Torres-Ruiz, J.M., Flexas, J., Fernández, J.E., Sebastiani, L., Diaz-Espejo, A., 2014. Regulation of photosynthesis and stomatal and mesophyll conductance under water stress and recovery in olive trees: correlation with gene expression of carbonic anhydrase and aquaporins. J. Exp. Bot. 65, 3143–3156. https://doi.org/10.1093/jxb/eru160.

Peters, W., van der Velde, I.R., van Schaik, E., Miller, J.B., Ciais, P., Duarte, H.F., van der Laan-Luijkx, I.T., van der Molen, M.K., Scholze, M., Schaefer, K., Vidale, P.L., Verhoef, A., Wårlind, D., Zhu, D., Tans, P.P., Vaughn, B., White, J.W.C., 2018. Increased water-use efficiency and reduced CO2 uptake by plants during droughts at a continental scale. Nat. Geosci. 11, 744–748. https://doi.org/10.1038/s41561-018-0212-7.

Pinheiro, C., Chaves, M.M., 2011. Photosynthesis and drought: can we make metabolic connections from available data? J. Exp. Bot. 62, 869–882. https://doi.org/10.1093/jxb/erq340.

Raes, D., Steduto, P., Hsiao, T.C., Fereres, E., 2018. Reference Manual Aquacrop (Version 6.0-6.1). AquaCrop. Website. http://www.fao.org/nr/water/aquacrop.html.

Ramírez, D.A., Yactayo, W., Rens, L.R., Rolando, J.L., Palacios, S., De Mendiburu, F., Mares, V., Barreda, C., Loayza, H., Monneveux, P., Zotarelli, L., Khan, A., Quiroz, R., 2016. Defining biological thresholds associated to plant water status for monitoring water restriction effects: stomatal conductance and photosynthesis recovery as key indicators in potato. Agric. Water Manage. 177, 369–378. https://doi.org/10.1016/j.agwat.2016.08.028.

Reichstein, M., Bahn, M., Ciais, P., Frank, D., Mahecha, M.D., Seneviratne, S.I., Zscheischler, J., Beer, C., Buchmann, N., Frank, D.C., Papale, D., Rammig, A., Smith, P., Thonicke, K., van der Velde, M., Vicca, S., Walz, A., Wattenbach, M., 2013. Climate extremes and the carbon cycle. Nature 500, 287–295. https://doi.org/10.1038/nature12350.

Reichstein, M., Falge, E., Baldocchi, D., Papale, D., Aubinet, M., Berbigier, P., Bernhofer, C., Buchmann, N., Gilmanov, T., Granier, A., Grunwald, T., Havrankova, K., Ilvesniemi, H., Janous, D., Knohl, A., Laurila, T., Lohila, A., Loustau, D., Matteucci, G., Meyers, T., Miglietta, F., Ourcival, J.-M., Pumpanen, J., Rambal, S., Rotenberg, E., Sanz, M., Tenhunen, J., Seufert, G., Vaccari, F., Vesala, T., Yakir, D., Valentini, R., 2005. On the separation of net ecosystem exchange into assimilation and ecosystem respiration: review and improved algorithm. Glob. Change Biol. 11, 1424–1439. https://doi.org/10.1111/j.1365-2486.2005.001002.x.

Reinhardt, K., Smith, W.K., 2008. Impacts of cloud immersion on microclimate, photosynthesis and water relations of Abies fraseri (Pursh.) Poiret in a temperate mountain cloud forest. Oecologia 158, 229–238. https://doi.org/10.1007/s00442-008-1128-5.

Rogers, A., Medlyn, B.E., Dukes, J.S., Bonan, G., von Caemmerer, S., Dietze, M.C., Kattge, J., Leakey, A.D.B., Mercado, L.M., Niinemets, Ü., Prentice, I.C., Serbin, S.P., Sitch, S., Way, D.A., Zaehle, S., 2017. A roadmap for improving the representation of photosynthesis in Earth system models. New Phytol. 213, 22–42. https://doi.org/10.1111/nph.14283.

Sands, P.J., Hackett, C., Nix, H.A., 1979. A model of the development and bulking of potatoes (Solanum Tuberosum L.) I. Derivation from well-managed field crops. Field Crops Res. 2, 309–331. https://doi.org/10.1016/0378-4290(79)90031-5.

Silva-Díaz, C., Ramírez, D.A., Rodríguez-Delfín, A., De Mendiburu, F., Rinza, J., Ninanya, J., Loayza, H., Quiroz, R., 2020. Unraveling Ecophysiological Mechanisms in Potatoes under Different Irrigation Methods: a Preliminary Field Evaluation. Agronomy 10, 827. https://doi.org/10.3390/agronomy10060827.

Singh, G., 1969. A review of the soil-moisture relationship in potatoes. Am Potato J 46, 398–403. https://doi.org/10.1007/BF02869560.

Spearman, C., 1904. The Proof and Measurement of Association between Two Things. Am. J. Psychol. 15, 72. https://doi.org/10.2307/1412159.

Stalham, M.A., Allen, E.J., 2004. Water uptake in the potato (Solanum tuberosum) crop. J. Agric. Sci. 142, 373–393. https://doi.org/10.1017/S0021859604004551.

Thom, A.S., 1972. Momentum, mass and heat exchange of vegetation. Q.J Royal Met. Soc. 98, 124–134. https://doi.org/10.1002/qj.49709841510.

Trugman, A.T., Medvigy, D., Mankin, J.S., Anderegg, W.R.L., 2018. Soil moisture stress as a major driver of carbon cycle uncertainty. Geophys. Res. Lett. 45, 6495–6503. https://doi.org/10.1029/2018GL078131.

Urban, J., Ingwers, M.W., McGuire, M.A., Teskey, R.O., 2017. Increase in leaf temperature opens stomata and decouples net photosynthesis from stomatal conductance in Pinus taeda and Populus deltoides x nigra. J. Exp. Bot. 68, 1757–1767. https://doi.org/10.1093/jxb/erx052.

Verhoef, A., Egea, G., 2014. Modeling plant transpiration under limited soil water: comparison of different plant and soil hydraulic parameterizations and preliminary implications for their use in land surface models. Agric. For. Meteorol. 191, 22–32. https://doi.org/10.1016/j.agrformet.2014.02.009.

Vidale, P.L., Egea, G., McGuire, P.C., Todt, M., Peters, W., Müller, O., Balan-Sarojini, B., Verhoef, A., 2021. On the treatment of soil water stress in GCM simulations of vegetation physiology. Front. Environ. Sci. 9, 689301 https://doi.org/10.3389/fenvs.2021.689301.

Wang, X., Du, T., Huang, J., Peng, S., Xiong, D., 2018. Leaf hydraulic vulnerability triggers the decline in stomatal and mesophyll conductance during drought in rice. J. Exp. Bot. 69, 4033–4045. https://doi.org/10.1093/jxb/ery188.

Wong, S.C., Cowan, I.R., Farquhar, G.D., 1979. Stomatal conductance correlates with photosynthetic capacity. Nature 282, 424–426. https://doi.org/10.1038/282424a0.

Yu, Z., Wang, J., Liu, S., Rentch, J.S., Sun, P., Lu, C., 2017. Global gross primary productivity and water use efficiency changes under drought stress. Environ. Res. Lett. 12, 014016 https://doi.org/10.1088/1748-9326/aa5258.

Zait, Y., Schwartz, A., 2018. Climate-related limitations on photosynthesis and drought-resistance strategies of Ziziphus spina-christi. Front. Forest. Glob. Chang. 1 https://doi.org/10.3389/ffgc.2018.00003.

Zhou, S., Duursma, R.A., Medlyn, B.E., Kelly, J.W.G., Prentice, I.C., 2013. How should we model plant responses to drought? An analysis of stomatal and non-stomatal responses to water stress. Agric. For. Meteorol. 182–183, 204–214. https://doi.org/10.1016/j.agrformet.2013.05.009.

Zhou, S., Medlyn, B., Sabaté, S., Sperlich, D., Prentice, I.C., Whitehead, D., 2014. Short-term water stress impacts on stomatal, mesophyll and biochemical limitations to photosynthesis differ consistently among tree species from contrasting climates. Tree Physiol. 34, 1035–1046. https://doi.org/10.1093/treephys/tpu072.

Zhu, K., Yuan, F.H., Wang, A.Z., Wu, J.B., Guan, D.X., Jin, C.J., Flexas, J., Gong, C.J., Zhang, H.X., Zhang, Y.S., 2021. Stomatal, mesophyll and biochemical limitations to soil drought and rewatering in relation to intrinsic water-use efficiency in Manchurian ash and Mongolian oak. Photosynt. https://doi.org/10.32615/ps.2020.084.